Null-Steering Beamformer-Based Feedback Cancellation for Multi-Microphone Hearing Aids With Incoming Signal Preservation

Henning Schepker, *Member, IEEE*, Sven Erik Nordholm, *Senior Member, IEEE*, Linh Thi Thuc Tran, *Student Member, IEEE*, and Simon Doclo, *Senior Member, IEEE*

***Abstract*—In hearing aids, acoustic feedback occurs due to the coupling between the hearing aid loudspeaker and microphone(s). In order to reduce the acoustic feedback, adaptive filters are commonly used to estimate the feedback contribution in the microphone(s). While theoretically allowing for perfect feedback cancellation, in practice the adaptive filter converges to an optimal solution that is typically biased due to the closed-loop acoustical system of the hearing aid. In order to avoid the adaptation to a biased optimal solution, in this paper we propose to use a fixed beamformer to cancel the acoustic feedback contribution for an earpiece with multiple integrated microphones and loudspeakers. By steering a spatial null in the direction of the hearing aid loudspeaker, we show that theoretically perfect feedback cancellation can be achieved. While previous null-steering beamforming approaches did not control for distortions of the incoming signal, in this paper we propose to incorporate a constraint based on the relative transfer function (RTF) of the incoming signal, aiming to perfectly preserve this signal. We formulate the computation of the beamformer coefficients both as a least-squares optimization procedure, aiming to minimize the residual feedback power, and as a min–max optimization procedure, aiming to directly maximize the maximum stable gain of the hearing aid. Experimental results using measured acoustic feedback paths from a custom earpiece with two microphones in the vent and a third microphone in the concha show that the proposed fixed null-steering beamformer using the RTF-based constraint provides a reduction of the acoustic feedback and substantially increases the added stable gain while preserving the incoming signal. This can even be achieved for unknown acoustic feedback paths and incoming signal directions.**

***Index Terms*—Acoustic feedback cancellation, least-squares optimization, min-max optimization, hearing aids, null-steering.**

Manuscript received September 3, 2018; revised January 2, 2019; accepted January 2, 2019. Date of publication January 10, 2019; date of current version February 15, 2019. This work was supported in part by the Deutsche Forschungsgemeinschaft (DFG, German Research Foundation)—Projektnummer 352015383—SFB 1330 C1, in part by the Research Unit FOR 1732 "Individualized Hearing Acoustics," and in part by the Cluster of Excellence 1077 "Hearing4all." The associate editor coordinating the review of this manuscript and approving it for publication was Prof. Richard Christian Hendriks. *(Corresponding author: Henning Schepker.)*

H. Schepker and S. Doclo are with the Signal Processing Group, Department of Medical Physics and Acoustics, University of Oldenburg, Oldenburg 26111, Germany (e-mail: henning.schepker@uni-oldenburg.de; simon.doclo@uni-oldenburg.de).

S. E. Nordholm and L. T. T. Tran are with the Faculty of Science and Engineering, Curtin University, Bentley, WA 6845, Australia (e-mail: S.Nordholm@curtin.edu.au; t.tran57@postgrad.curtin.edu.au).

Digital Object Identifier 10.1109/TASLP.2019.2892234

I. Introduction

Due to the acoustic coupling between the hearing aid loudspeaker and microphone(s), acoustic feedback is a common problem limiting the maximum applicable gain in hearing aids. Most often acoustic feedback is perceived as whistling or howling. In order to reduce the acoustic feedback in changing acoustics and to increase the maximum gain that can be applied in the hearing aid, robust feedback suppression strategies are required.

Different approaches exist to reduce the acoustic feedback, e.g., feedforward suppression algorithms, acoustic feedback cancellation (AFC) algorithms and spatial filtering algorithms (see also [1]). On the one hand, feedforward suppression algorithms typically modify the loudspeaker signal and thus provide a trade-off between a limited feedback reduction performance and perceptually audible distortions. On the other hand, AFC algorithms use an adaptive filter to model the acoustic feedback path(s) between the hearing aid loudspeaker and the microphone(s) [1]–[8]. In theory using a filter to model the acoustic feedback path allows for perfect cancellation of the acoustic feedback. However, due to the closed-loop acoustical system of the hearing aid, the optimal filter solution to which the adaptive filter is converging is usually biased, e.g., [3], [9]. Different approaches have been proposed to reduce the bias, e.g., by using the so-called prediction-error-method (PEM) [2], [3], [10], by using an additional probe noise [4], [5] or by using phase modulation and frequency shifting [11]. In addition, it has been shown that an improved reduction of the bias can be achieved by exploiting an additional microphone, e.g., in multi-microphone hearing aids, by adaptively removing the contribution of the incoming signal in the filter adaptation [12], [13]. Using spatial filtering algorithms it is possible to reduce the (directional) acoustic feedback contribution in the microphones, e.g., by using a combined multi-microphone feedback cancellation and noise reduction scheme [14], [15]. Additionally, spatial filtering algorithms allow to avoid the adaptation towards a biased optimal solution completely by using a fixed, i.e., time-invariant, beamformer to reduce the feedback contribution in the microphones [16]–[18].

In this paper we consider a custom multi-microphone hearing aid and propose to cancel the acoustic feedback using a fixed null-steering beamformer, thus avoiding the problem of

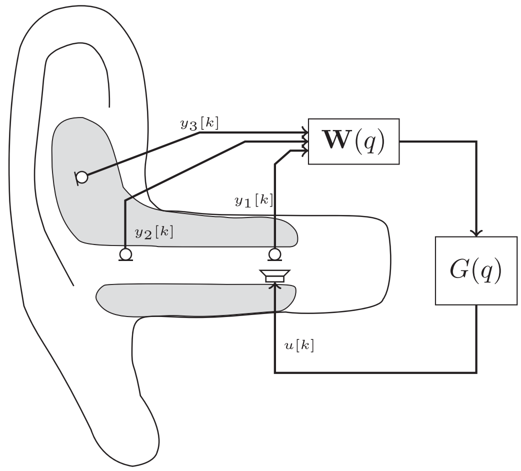

Fig. 1. Considered hearing aid setup with a single-loudspeaker three-microphone earpiece.

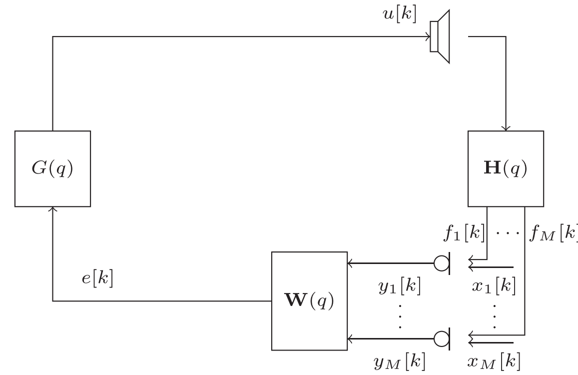

Fig. 2. Generic single-loudspeaker multi-microphone closed-loop hearing aid system.

adapting to a typically biased optimal solution. In particular, we consider a custom earpiece [19], [20] (see Fig. 1) with two closely spaced microphones and a loudspeaker in the vent, and a third microphone located in the concha. In contrast to conventional behind-the-ear hearing aids, this earpiece design allows to design a fixed beamformer with a spatial null in the direction of the hearing aid loudspeaker located in the vent [16]–[18]. Thus, the null-steering beamformer ideally cancels all signals originating from the hearing aid receiver and does not impact the incoming (external) signal. Similarly as in [16], [17] and [18], we propose to compute the null-steering beamformer to either minimize the residual feedback power or maximize the maximum stable gain (MSG). However, in those studies only a constraint on the null-steering beamformer was considered where the coefficients in a reference microphone were chosen to be fixed delay and hence did not directly control for any distortions of the incoming signal. In contrast, in this paper we propose to incorporate a constraint based on the relative transfer function (RTF) of the incoming signal in order to directly preserve the incoming signal in the beamformer output. Furthermore, when maximizing the maximum stable gain using a linear programming (LP) formulation, in [18] the real and imaginary parts of the frequency response of the beamformer output were assumed to be independent of each other. In fact, this approximates the desired circular cost of the involved min-max optimization problem by using a squared box cost, hence possibly leading to suboptimal performance. In this paper we extend this optimization by using the so-called real rotation theorem [21] allowing to approximate the desired optimization problem with arbitrarily small error.

In this paper we propose the three following extensions to previous work:

1) to use a constraint based on the RTF of the incoming signal.
2) to formulate the optimization of the beamformer coefficients as a min-max optimization program aiming to maximize the maximum stable gain, where we use the real rotation theorem [21] to extend the optimization approach proposed in [18].
3) to provide an extensive experimental comparison of the null-steering beamformer minimizing the residual feedback power and the null-steering beamformer maximizing the maximum stable gain of the hearing aid.

Experimental results using measured acoustic feedback paths show that the proposed null-steering beamformer provides a substantial reduction of the acoustic feedback, while preserving a high perceptual speech quality even for different unknown incoming source directions. Furthermore, the fixed beamformer also enables to increase the added stable gain for challenging acoustic conditions, i.e., after repositioning of the earpiece and with a telephone receiver close to the ear. In addition, when combined with a PEM-AFC algorithm, experimental results show that the proposed null-steering beamformer and the PEM-AFC algorithm provide complementary performance, i.e., the performance in terms of the MSG of the combination is similar to the sum of the MSGs (in dB) of the individual algorithms.

This paper is organized as follows. In Section II the considered acoustic scenario and general notation are introduced. In Section III we analyse the considered single-loudspeaker multi-microphone hearing aid system and show that in theory perfect feedback cancellation can be achieved using a null-steering beamformer. In Section IV the computation of the beamformer coefficients is formulated both as linearly constrained least-squares optimization problems to reduce the residual feedback power and linearly constrained min-max optimization problems to maximize the MSG. In Section V the different fixed null-steering beamformer solutions are evaluated using measured acoustic feedback paths from a custom multi-microphone earpiece with three microphones and one loudspeaker.

II. Acoustic Scenario and Notation

Consider a single-loudspeaker multi-microphone hearing aid system with M microphones as depicted in Fig. 2. For simplicity we assume that all transfer functions are linear and time-invariant.

The mth microphone signal $y_m[k]$, $m = 1, \ldots, M$, at discrete time k is the sum of the incoming signal $x_m[k]$ and the loudspeaker contribution in the mth microphone $f_m[k]$, i.e.,

$$y_m[k] = x_m[k] + f_m[k] \tag{1}$$

$$= x_m[k] + H_m(q)u[k], \tag{2}$$

where $u[k]$ denotes the loudspeaker signal and $H_m(q)$ denotes the acoustic feedback path between the mth microphone and the loudspeaker. We assume that the acoustic feedback path can be modelled as an L_H-dimensional polynomial in q, i.e.,

$$H_m(q) = h_{m,0} + \cdots + h_{m,L_H-1}q^{-L_H+1}, \tag{3}$$

$$= \mathbf{h}_m^T \mathbf{q}, \tag{4}$$

where $[\cdot]^T$ denotes transpose operation, $\mathbf{q}$ is the vector containing the delay-elements of q of appropriate length and $\mathbf{h}_m$ denotes the impulse response of the mth acoustic feedback path, i.e.,

$$\mathbf{h}_m = \begin{bmatrix} h_{m,0} & \dots & h_{m,L_H-1} \end{bmatrix}^T. \tag{5}$$

By stacking all microphone signals into an M-dimensional vector, (2) can be rewritten as

$$\mathbf{y}[k] = \mathbf{x}[k] + \mathbf{H}(q)u[k], \tag{6}$$

with

$$\mathbf{y}[k] = \begin{bmatrix} y_1[k] & \dots & y_M[k] \end{bmatrix}^T, \tag{7}$$

$$\mathbf{x}[k] = \begin{bmatrix} x_1[k] & \dots & x_M[k] \end{bmatrix}^T, \tag{8}$$

$$\mathbf{H}(q) = \begin{bmatrix} H_1(q) & \dots & H_M(q) \end{bmatrix}^T. \tag{9}$$

After applying a fixed filter-and-sum beamformer to the microphone signals the beamformer output signal $e[k]$ is obtained, i.e.,

$$e[k] = \mathbf{W}^T(q)\mathbf{y}[k], \tag{10}$$

$$= \underbrace{\mathbf{W}^T(q)\mathbf{x}[k]}_{\tilde{x}[k]} + \underbrace{\mathbf{W}^T(q)\mathbf{f}[k]}_{\tilde{f}[k]}, \tag{11}$$

where $\mathbf{W}(q)$ denotes the M-dimensional vector of the beamformer weighting functions and $\mathbf{f}[k]$ denotes the M-dimensional vector of the feedback component in the microphones, i.e.,

$$\mathbf{W}(q) = \begin{bmatrix} W_1(q) & \dots & W_M(q) \end{bmatrix}^T, \tag{12}$$

$$\mathbf{f}[k] = \begin{bmatrix} f_1[k] & \dots & f_M[k] \end{bmatrix}^T, \tag{13}$$

and $\tilde{x}[k]$ and $\tilde{f}[k]$ are the residual incoming signal and residual feedback component, respectively. The L_W-dimensional beamformer coefficient vector of $W_m(q)$ for the mth microphone is defined as

$$\mathbf{w}_m = \begin{bmatrix} w_{m,0} & \dots & w_{m,L_W-1} \end{bmatrix}^T, \tag{14}$$

and the ML_W-dimensional stacked vector of the beamformer coefficient vectors is defined as

$$\mathbf{w} = \begin{bmatrix} \mathbf{w}_1^T & \dots & \mathbf{w}_M^T \end{bmatrix}^T. \tag{15}$$

The signal $e[k]$ is then processed using the hearing aid forward path $G(q)$, yielding the loudspeaker signal $u[k]$, i.e.,

$$u[k] = G(q)e[k]. \tag{16}$$

Moreover, we assume that the incoming signal $\mathbf{x}[k]$ is composed of a single directional speech source $s[k]$, i.e.,

$$\mathbf{x}[k] = \mathbf{D}(q)s[k], \tag{17}$$

where $\mathbf{D}(q)$ is the M-dimensional vector containing the acoustic transfer function between the source and each of the M microphones, i.e.,

$$\mathbf{D}(q) = \begin{bmatrix} D_1(q) & \dots & D_M(q) \end{bmatrix}^T. \tag{18}$$

The L_D-dimensional impulse response vector of the acoustic transfer function for the mth microphone is defined as

$$\mathbf{d}_m = \begin{bmatrix} d_{m,0} & \dots & d_{m,L_D-1} \end{bmatrix}^T. \tag{19}$$

The incoming signal $\mathbf{x}[k]$ can also be defined by using the relative transfer function (RTF) between a reference microphone m_0 and the remaining microphones, i.e.,

$$\mathbf{x}[k] = \tilde{\mathbf{D}}(q)x_{m_0}[k] = \tilde{\mathbf{D}}(q)D_{m_0}(q)s[k], \tag{20}$$

where $\tilde{\mathbf{D}}(q)$ is the M-dimensional vector containing the RTF between the microphones, i.e.,

$$\tilde{\mathbf{D}}(q) = \frac{\mathbf{D}(q)}{D_{m_0}(q)}, \tag{21}$$

with $D_{m_0}(q)$ the acoustic transfer function between the source and the reference mirophone m_0. The $L_{\tilde{D}}$-dimensional impulse response vector of the relative transfer function for the mth microphone is defined as

$$\tilde{\mathbf{d}}_m = \begin{bmatrix} \tilde{d}_{m,0} & \dots & \tilde{d}_{m,L_{\tilde{D}}-1} \end{bmatrix}^T. \tag{22}$$

Furthermore, the beamformer response for the acoustic feedback paths in the frequency domain at discrete angular frequency ω_n can be computed by applying the N_{FFT}-point discrete Fourier transform (DFT) to the beamformer response in the time-domain, i.e.,

$$\mathbf{H}^H(\omega_n)\mathbf{W}(\omega_n) = \mathfrak{f}^T(\omega_n)\mathbf{H}\mathbf{w}, \tag{23}$$

where $\mathfrak{f}(\omega_n)$ is the $(L_H + L_W - 1)$-dimensional vector of the DFT matrix, i.e.,

$$\mathfrak{f}(\omega_n) = \begin{bmatrix} 1 & e^{-\frac{j2\pi n}{N_{FFT}}} & e^{-\frac{j2\pi 2n}{N_{FFT}}} & \dots & e^{-\frac{j2\pi n(L_H+L_W-2)}{N_{FFT}}} \end{bmatrix}^T, \tag{24}$$

and $\mathbf{H}$ is the $(L_H + L_W - 1) \times ML_W$-dimensional matrix of the concatenated $(L_H + L_W - 1) \times L_W$-dimensional convolution matrices $\mathbf{H}_m$, i.e.,

$$\mathbf{H} = \begin{bmatrix} \mathbf{H}_1 & \dots & \mathbf{H}_M \end{bmatrix}, \tag{25}$$

with

$$\mathbf{H}_m = \begin{bmatrix} h_{m,0} & 0 & \dots & 0 \\ h_{m,1} & h_{m,0} & \ddots & \vdots \\ \vdots & \ddots & \ddots & \vdots \\ h_{m,L_W-1} & \ddots & \ddots & h_{m,0} \\ \vdots & \ddots & \ddots & \vdots \\ h_{m,L_H-1} & \ddots & \ddots & \vdots \\ \vdots & \ddots & \ddots & \vdots \\ 0 & \dots & \dots & h_{m,L_H-1} \end{bmatrix}. \quad (26)$$

III. System Analysis

In the following we analyse the transfer function of the hearing aid system depicted in Fig. 2. By combining (6), (10), and (16) we can rewrite the loudspeaker signal as

$$u[k] = G(q)\mathbf{W}^T(q)\mathbf{x}[k] + G(q)\mathbf{W}^T(q)\mathbf{H}(q)u[k], \quad (27)$$

such that

$$u[k] = \underbrace{\frac{G(q)\mathbf{W}^T(q)}{1 - O(q)}}_{\mathbf{C}^T(q)}\mathbf{x}[k], \quad (28)$$

with $\mathbf{C}(q)$ the closed-loop transfer function and $O(q)$ the open-loop transfer function defined as

$$O(q) = G(q)\mathbf{W}^T(q)\mathbf{H}(q). \quad (29)$$

From this expression it can be observed that perfect feedback cancellation for the considered system can be achieved under the following condition: The beamformer $\mathbf{W}(q)$ cancels the feedback contribution in the microphones, i.e.,

$$\mathbf{W}^T(q)\mathbf{H}(q) = 0, \quad (30)$$

with $W_m(q) \neq 0$ for at least one $m \in [1, \dots, M]$ to avoid the trivial solution.

Furthermore, if (30) holds, then from (28) and using (17) we obtain

$$u[k] = G(q)\mathbf{W}^T(q)\mathbf{x}[k] \quad (31)$$

$$= G(q)\mathbf{W}^T(q)\mathbf{D}(q)s[k]. \quad (32)$$

Note that although (30) provides a perfect solution to the feedback cancellation problem, applying the beamformer coefficients will hence also modify the incoming signals $\mathbf{x}[k]$, possibly leading to sound quality degradation.

Assuming a broadband forward path gain function $G(q) = |G|q^{-d_G}$ with $d_G \geq 1$ a delay, the maximum stable gain $\mathcal{M}_i$ of the closed-loop system for the ith set of acoustic feedback path measurements can be obtained by rearranging the magnitude response of the open-loop transfer function $|O(\omega_n)| = 1$ for the broadband gain $|G|$, i.e.,

$$\mathcal{M}_i = \frac{1}{\max_{\omega_n} |(\mathbf{H}^{(i)})^H(\omega_n)\mathbf{W}(\omega_n)|^2}. \quad (33)$$

Note that in (33) it is assumed that the phase of the open-loop transfer function is a multiple of 2π for all frequencies ω_n, hence providing a worst-case assumption for the MSG. Assuming that for different sets of measurements of the acoustic feedback paths the lowest MSG determines the MSG of the hearing aid in challenging conditions we further define the *overall MSG* as

$$\mathcal{M} = \min_i \mathcal{M}_i. \quad (34)$$

IV. Fixed Null-Steering Beamformer Design

In this section we consider the design of a fixed null-steering beamformer to cancel the feedback contribution of the loudspeaker in the microphones. In order to compute the fixed null-steering beamformer, we assume knowledge of multiple (I) sets of acoustic feedback paths $\mathbf{H}^{(i)}(q)$, $i = 1, \dots, I$, e.g., by measurement. Furthermore, we assume knowledge of the acoustic transfer functions $\mathbf{D}(q)$ between the source and the microphones or their corresponding RTF $\tilde{\mathbf{D}}(q)$. We assume that in a practical scenario all computations required to compute the null-steering beamformer can be performed offline and the obtained filter coefficients are then transferred to the hearing device. In Section IV-A we present the different objective functions and in Section IV-B we present the existing fixed delay constraint and the proposed RTF-based constraint. In Section IV-C and IV-D we formulate the computation of the null-steering subject to the different constraints as least-squares optimization problems and min-max optimization problems, respectively.

A. Objective Functions

To compute the beamformer coefficient vector $\mathbf{w}$ we use two different cost functions, aiming at either minimizing the residual feedback power or maximizing the MSG. On the one hand, minimizing the *average residual feedback power* across several (I) sets of acoustic feedback path measurements corresponds to minimizing the least-squares error of the beamformer, i.e., the least-squares cost function

$$J_{LS}(\mathbf{w}) = \sum_{i=1}^{I} \|\mathbf{H}^{(i)}\mathbf{w}\|_2^2, \quad (35)$$

where $\mathbf{H}^{(i)}$ is the convolution matrix of the acoustic feedback paths for the ith set of measurements, $i = 1, \dots, I$, defined similarly as $\mathbf{H}$ in (25).

On the other hand, similarly as in [22] for the optimization of a common part of acoustic feedback paths, maximizing the *overall MSG* in (34) in a multi-microphone hearing aid corresponds to minimizing the denominator in (33) across all measurements $i = 1, \dots, I$, i.e., the following cost function

$$J_{MM}(\mathbf{w}) = \max_{i,\omega_n} |\mathbf{H}^{(i),H}(\omega_n)\mathbf{W}(\omega_n)|^2, \quad (36)$$

where $\mathbf{H}^{(i)}(\omega_n)$ is the M-dimensional vector of the frequency response of the acoustic feedback path at frequency ω_n for the ith measurement, defined similarly as $\mathbf{H}(\omega_n)$ in (23).

B. Constraints

Note that both cost functions (35) and (36) can be minimized by $\mathbf{w} = \mathbf{0}$, which is obviously not desired since this would result in $u[k] = e[k] = 0$. Therefore, in this section we first present the *fixed delay constraint* used in [7], [16], [18] and then propose an *RTF constraint* based on the RTF of the incoming signal to mitigate this trivial solution.

The *fixed delay constraint* sets the beamformer coefficients in the reference microphone m_0 equal to a delay of L_d samples, i.e.,

$$\mathbf{w}_{m_0} = [\underbrace{0 \; \dots \; 0}_{L_d} \; 1 \; 0 \; \dots \; 0]^T = \check{\mathbf{e}}_{L_d}, \tag{37}$$

where we use $\check{\mathbf{e}}_{L_d}$ to denote a vector of appropriate length with its (L_d+1)th element equal to 1. Note that applying this constraint does not control for distortions of the incoming signal. Therefore, we propose a constraint that directly preserves the incoming signal in a reference microphone in the beamformer output, i.e., $\tilde{x}[k] = x_{m_0}[k]$. Applying the beamformer to the incoming signal $\mathbf{x}[k]$ in (17) the beamformer output for the incoming signal yields $\tilde{x}[k] = \mathbf{W}^T(q)\mathbf{D}(q)s[k]$. Similarly, this can be done for the definition of the incoming signal $\mathbf{x}[k]$ in (20) using the RTF where the beamformer output for the incoming signal yields $\tilde{x}[k] = \mathbf{W}^T(q)\tilde{\mathbf{D}}(q)x_{m_0}[k]$. Hence, if the beamformer output for the RTF of the incoming signal yields a unit (or a delayed unit) response, i.e.,

$$\mathbf{W}^T(q)\tilde{\mathbf{D}}(q) = q^{-L_d}, \tag{38}$$

the incoming signal is preserved. This can be formulated in the time-domain as

$$\boxed{\tilde{\mathbf{D}}\mathbf{w} = \check{\mathbf{e}}_{L_d}} \tag{39}$$

where $\tilde{\mathbf{D}}$ is the $(L_{\tilde{D}} + L_W - 1) \times ML_W$-dimensional matrix of concatenated $(L_{\tilde{D}} + L_W - 1) \times L_W$ convolution matrices $\tilde{\mathbf{D}}_m$, i.e.,

$$\tilde{\mathbf{D}} = \left[\, \tilde{\mathbf{D}}_1 \quad \dots \quad \tilde{\mathbf{D}}_M \,\right], \tag{40}$$

where $\tilde{\mathbf{D}}_m$ is defined similarly as $\mathbf{H}_m$ in (26). Note that although different methods exist to compute the RTFs, in this paper we consider a simple regularized least-squares optimization method (cf. Appendix).

C. Least-Squares Optimization

By combining the least-squares cost function in (35) with the fixed delay constraint in (37) we obtain the following linearly constrained least-squares optimization problem

$$\boxed{\begin{aligned} &\min_{\mathbf{w}} \quad \sum_{i=1}^{I} \|(\mathbf{H}^{(i)})\mathbf{w}\|_2^2 && \text{(41a)}\\ &\text{subject to} \quad \mathbf{w}_{m_0} = \check{\mathbf{e}}_{L_d} && \text{(41b)} \end{aligned}}$$

By substituting the constraint directly in the cost function this optimization problem can be reformulated as

$$\min_{\mathbf{w}} \quad \sum_{i=1}^{I} \|(\mathbf{H}_{m_0}^{(i)})\check{\mathbf{e}}_{L_d} + \sum_{\substack{m=1\\ m\neq m_0}}^{M} (\mathbf{H}_m^{(i)})\mathbf{w}_m\|_2^2. \tag{42}$$

The closed-form solution to this optimization problem is given by

$$\check{\mathbf{w}} = (\bar{\mathbf{H}}^T\bar{\mathbf{H}})^{-1}\bar{\mathbf{H}}^T\bar{\mathbf{H}}_{m_0}\check{\mathbf{e}}_{L_d}, \quad \mathbf{w}_{m_0} = \check{\mathbf{e}}_{L_d}, \tag{43}$$

where $\bar{\mathbf{H}}$ is the $I(L_W + L_H - 1) \times (M-1)L_W$-dimensional matrix of stacked and concatenated convolution matrices $\mathbf{H}_m^{(i)}$, $m = 1, \dots, M$, $m \neq m_0$, $i = 1, \dots, I$ in (26) and $\bar{\mathbf{H}}_{m_0}$ is the $I(L_W + L_H - 1) \times L_W$-dimensional matrix of stacked matrices $\mathbf{H}_{m_0}^{(i)}$, $i = 1, \dots, I$.

When using the proposed RTF-based constraint in (39) instead of the fixed delay constraint in (37), the optimization problem can be formulated using multiple (J) RTF constraints, e.g., to constrain multiple incoming signal directions, leading to a similar linearly constrained least-squares problem as in (41), i.e.,

$$\boxed{\begin{aligned} &\min_{\mathbf{w},i} \quad \sum_{i=1}^{I} \|(\mathbf{H}^{(i)})\mathbf{w}\|_2^2 && \text{(44a)}\\ &\text{subject to} \quad \tilde{\mathbf{D}}^{(j)}\mathbf{w} = \check{\mathbf{e}}_{L_d} \quad \forall j = 1, \dots, J && \text{(44b)} \end{aligned}}$$

where the convolution matrix $\tilde{\mathbf{D}}^{(j)}$ for the jth RTF measurement is defined similarly as $\tilde{\mathbf{D}}$ in (40).

Note that for the fixed delay constraint in (41) the filter coefficients in the reference microphone are constrained to be a delay, whereas for the RTF-based constraint in (44) the response of the beamformer for a specific incoming signal direction is constrained to be a delay.

The closed-form solution of this optimization problem is given by

$$\mathbf{w} = (\tilde{\mathbf{H}}^T\tilde{\mathbf{H}})^{-1}\bar{\mathbf{D}}^T(\bar{\mathbf{D}}(\tilde{\mathbf{H}}^T\tilde{\mathbf{H}})^{-1}\bar{\mathbf{D}}^T)^{-1}\bar{\mathbf{e}}_{L_d}, \tag{45}$$

where $\tilde{\mathbf{H}}$ is the $I(L_W + L_H - 1) \times ML_W$-dimensional matrix of stacked convolution matrices $\mathbf{H}^{(i)}$, $i = 1, \dots, I$ in (25), $\bar{\mathbf{D}}$ is the $J(L_{\tilde{D}} + L_W - 1) \times ML_W$-dimensional stacked convolution matrix of $\tilde{\mathbf{D}}^{(j)}$, $j = 1, \dots, J$, and $\bar{\mathbf{e}}_{L_d}$ is the $J(L_{\tilde{D}} + L_W - 1)$-dimensional vector of stacked vectors $\check{\mathbf{e}}_{L_d}$.

D. Min-Max Optimization

Instead of minimizing the residual feedback power using the least-squares optimization procedures in Section IV-C, in this section we formulate the optimization of the null-steering beamformer to directly maximize the overall MSG of the hearing aid defined in (34).

By combining the cost function in (36) with the fixed delay constraint in (37) we obtain the following linearly constrained min-max optimization problem

$$\boxed{\begin{aligned} &\min_{\mathbf{w}} \quad \max_{\omega_n, i} |(\mathbf{H}^{(i)})^H(\omega_n)\mathbf{W}(\omega_n)|^2 && \text{(46a)}\\ &\text{subject to} \quad \mathbf{w}_{m_0} = \check{\mathbf{e}}_{L_d} && \text{(46b)} \end{aligned}}$$

where $\mathbf{H}^{(i)}(\omega_n)$ is the M-dimensional vector containing the frequency responses of the acoustic feedback paths for the ith measurement.

Contrary to the least-squares optimization problem in (41), this min-max optimization problem does not have a closed-form solution. By introducing the non-negative auxiliary variable t [23], the optimization problem in (46) can be reformulated as

$$\min_{t,\mathbf{w}} \quad t \tag{47a}$$

$$\text{subject to} \quad |(\mathbf{H}^{(i)})^H(\omega_n)\mathbf{W}(\omega_n)|^2 \leq t \tag{47b}$$

$$\mathbf{w}_{m_0} = \check{\mathbf{e}}_{L_d}. \tag{47c}$$

By recognizing (47b) as a Schur complement [24], the optimization problem in (47) can be formulated as the following semidefinite programming (SDP) problem

$$\min_{t,\mathbf{w}} \quad t \tag{48a}$$

$$\text{subject to} \quad \begin{bmatrix} t & p^{(i)}(\omega_n) & q^{(i)}(\omega_n) \\ p^{(i)}(\omega_n) & 1 & 0 \\ q^{(i)}(\omega_n) & 0 & 1 \end{bmatrix} \succeq \mathbf{0}, \forall \omega_n, i \tag{48b}$$

$$\mathbf{w}_{m_0} = \check{\mathbf{e}}_{L_d}, \tag{48c}$$

where $\succeq \mathbf{0}$ denotes positive semidefiniteness, and $p^{(i)}(\omega_n)$ and $q^{(i)}(\omega_n)$ denote the real and the imaginary parts of the residual beamformer error for the ith measurement, i.e.,

$$p^{(i)}(\omega_n) = \mathfrak{Re}\{(\mathbf{H}^{(i)})^H(\omega_n)\mathbf{W}(\omega_n)\}, \tag{49}$$

$$q^{(i)}(\omega_n) = \mathfrak{Im}\{(\mathbf{H}^{(i)})^H(\omega_n)\mathbf{W}(\omega_n)\}. \tag{50}$$

The SDP problem in (48) can then be solved using existing convex optimization tools, e.g., as implemented in the convex optimization toolbox CVX [25], [26]. However, with an increasing number of frequencies and/or number of measurements it cannot be exactly solved using existing optimization tools due to the increasingly large scale of the optimization problem [26]. Therefore, we propose to approximate the optimization problem in (48) using the real rotation theorem [21] as an LP problem. Using the real rotation theorem [21] the aim is to approximate the minimization of the absolute value with arbitrarily small error by projecting the complex residual beamformer error onto a rotating complex pointer using a finite set of rotation angles. The optimization problem in (46) can thus be approximated as the following LP problem for all ω_n, ϕ_l and $i = 1, \ldots, I$

$$\min_{t,\mathbf{w}} \quad t \tag{51a}$$

$$\text{subject to} \quad p^{(i)}(\omega_n)\cos\phi_l + q^{(i)}(\omega_n)\sin\phi_l \leq t \tag{51b}$$

$$\mathbf{w}_{m_0} = \check{\mathbf{e}}_{L_d}, \tag{51c}$$

with ϕ_l the lth rotation angle, $l = 1, \ldots, N_\phi$. The approximation error when using (51) depends on the choice of N_ϕ [21] and is bounded for, e.g., a choice of $N_\phi = 4$ to approximately 3 dB and for $N_\phi = 16$ to approximately 0.17 dB. Note that the optimization problem formulated in [18] corresponds to the special case of $N_\phi = 4$.

When using the RTF-based constraint in (39) we additionally aim at avoiding distortions of the incoming signal by considering multiple (J) RTF measurements. The design of the null-steering beamformer using the proposed RTF-based constraint in (39) can then be formulated as the following linearly constrained min-max optimization problem

$$\boxed{\begin{aligned} &\min_{\mathbf{w}} \quad \max_{\omega_n, i} |(\mathbf{H}^{(i)})^H(\omega_n)\mathbf{W}(\omega_n)|^2 && (52a) \\ &\text{subject to} \quad \tilde{\mathbf{D}}^{(j)}\mathbf{w} = \check{\mathbf{e}}_{L_d} \ \ \forall j = 1, \ldots, J && (52b) \end{aligned}}$$

The optimization problem in (52) can be approximated as an LP problem using the real rotation theorem, i.e., for all ω_n, ϕ_l, $i = 1, \ldots, I$

$$\min_{t,\mathbf{w}} \quad t \tag{53a}$$

$$\text{subject to} \quad p^{(i)}(\omega_n)\cos\phi_l + q^{(i)}(\omega_n)\sin\phi_l \leq t, \tag{53b}$$

$$\tilde{\mathbf{D}}^{(j)}\mathbf{w} = \check{\mathbf{e}}_{L_d} \ \ \forall j = 1, \ldots, J. \tag{53c}$$

Both the linear program in (51) and the linear program in (53) can be solved using the convex optimization toolbox CVX [25], [26].

V. Experimental Evaluation

In this section the performance of the proposed RTF-constrained null-steering beamformer is evaluated when using 2 or 3 microphones and compared with the existing approaches [17], [18] that used the fixed delay constraint in (37). In particular, we consider the ability to cancel the acoustic feedback in different acoustic scenarios as well as the distortion of the incoming signal. In Section V-A we describe the acoustic setup and the used performance measures. In Section V-B we present experimental results to justify our selection of the parameters for the RTF constraint. In Section V-C the optimal performance of the null-steering beamformer is investigated, i.e., the same IRs were used for optimization and evaluation. In Section V-D the robustness against changes in the acoustic feedback paths is investigated, i.e., different IRs were used for optimization and evaluation. In Section V-E the perceptual quality and robustness against changes of the incoming signal direction is evaluated. Finally, in Section V-F we compare and combine the proposed null-steering beamformer with a PEM-AFC algorithm.

A. Setup and Performance Measures

Acoustic feedback paths and acoustic transfer functions were measured for the three-microphone-one-loudspeaker earpiece depicted in Fig. 1, which was inserted to the right ear of a dummy head with adjustable ear canals [27]. The IRs of the acoustic feedback paths and acoustic transfer functions were sampled at $f_s = 16$ kHz and truncated to length $L_H = 100$ and $L_D = 3000$. Measurements were performed in an acoustically treated chamber ($T_{60} \approx 300$ ms) and the distance between the external source and the dummy head was approximately 1.2 m (cf. experimental setup depicted in Fig. 3). Acoustic feedback

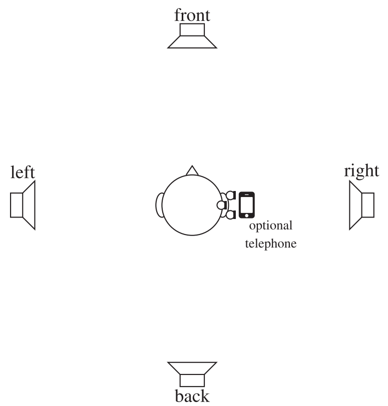

Fig. 3. Experimental setup used for the measurement of acoustic feedback paths and acoustic transfer functions. For conciseness the hearing aid loudspeaker is not shown.

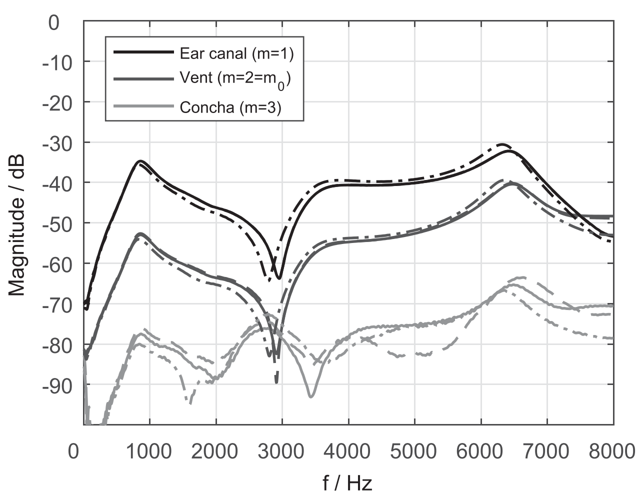

Fig. 4. Amplitude responses of the measured acoustic feedback paths. Continuous lines show feedback paths in free-field, i.e., without any obstruction (used for computing the beamformer coefficients), dashed dotted lines show exemplary responses after repositioning of the earpiece, and dashed lines show the acoustic feedback paths in the presence of a telephone receiver.

paths were measured in free-field, i.e., without any obstruction close to the ear, and with a telephone close to the ear. For both conditions ten measurements were performed, where after each measurement the earpiece was removed from the dummy head and reattached, leading to a total of twenty different feedback path measurements. Four different directions of the external source were considered: frontal, 90 degrees right, back, 90 degrees left. Fig. 4 shows the amplitude responses of the measured acoustic feedback paths for the three different microphones and for different acoustic conditions. The forward path of the hearing aid was set to $G(q) = q^{-96} 10^{45/20}$, corresponding to a delay of 6 ms and a broadband amplification of 45 dB. For all experiments the reference microphone $m_0 = 2$, i.e., the microphone located at the outer phase of the vent, was chosen since it includes most of the relevant spectral and directional cues and hence provides a natural position for sound pickup. For all min-max optimization procedures we use $N_{FFT} = 2048$ discrete frequencies and $N_\phi = 16$ rotation angles to approximate the desired cost function leading to an approximation error of 0.17 dB. For the optimization using the fixed delay constraint we used $L_d = L_W/2$ as suggested in [16], [17].

We evaluated the feedback cancellation performance of the null-steering beamformer using the added stable gain (ASG) [2], [29] and the perceptual quality of the signal after applying the null-steering beamformer using the narrow-band perceptual evaluation of speech quality (PESQ) measure [28].

The ASG for the considered hearing aid setup is computed as

$$ASG = 20 \log_{10} \frac{1}{\max_{\omega_n} |\mathbf{H}^H(\omega_n)\mathbf{W}(\omega_n)|} - MSG_{m_0}, \tag{54}$$

where MSG_{m_0} is the maximum stable gain of the hearing aid using only the reference microphone m_0, i.e.,

$$MSG_{m_0} = 20 \log_{10} \frac{1}{\max_{\omega_n} |H_{m_0}(\omega_n)|}. \tag{55}$$

The reference signal for the PESQ measure was the incoming signal $x_{m_0}[k]$ in the reference microphone, while the test signal was the error signal $e[k]$ after applying the beamformer. In order to assess only the effect of the beamformer on speech quality and avoid any influence of the acoustic feedback on the PESQ results, for the perceptual quality evaluation no hearing aid processing was applied, i.e., the hearing aid forward path was set to $G(q) = 0$, and hence $e[k] = \tilde{x}[k]$ in (11).[1] As speech source we used an 80 s long signal obtained by concatenating multiple sentences from the TIMIT database [30].

B. Experiment 1: Selection of RTF Parameters

In the first experiment we investigate the impact of the RTF length $L_{\tilde{D}}$ and the delay L_d in the RTF computation (cf. Appendix A) on the performance of the proposed RTF-based null-steering beamformer. Specifically we consider the least-squares optimization in (44) using ten sets of measurements of the acoustic feedback paths ($I = 10$) measured in free-field and a single acoustic transfer function of the incoming signal ($J = 1$, frontal direction). We use the same ten sets of acoustic feedback paths and one acoustic transfer functions for optimization and evaluation. Fig. 5 depicts exemplary results using $M = 2$ microphones in terms of the average ASG and the average PESQ mean opinion scores (MOS) as well as minimum and maximum ASG values and PESQ MOS as a function of the RTF length $L_{\tilde{D}}$ for a delay of $L_d = 0$ and a delay of $L_d = L_{\tilde{D}}/2$. As can be observed using $L_d = 0$ generally leads to a larger average ASG and larger average PESQ MOS values. Furthermore, the largest average ASG is obtained for $L_{\tilde{D}} = 8$, $L_d = 0$. Therefore, in the following experiments these values are used to compute the RTF used in the RTF constraint.

[1] Note that including the residual feedback component $\tilde{f}[k]$ in the evaluation of the PESQ measure requires a non-trivial choice of the forward path gain, which impacts the obtained results. If the gain is chosen too low, the feedback component has no impact on the results, while if the gain is chosen larger, it will mainly impact algorithms which result in a low MSG, e.g., an MSG that is 3 dB larger than the used gain. In order to avoid mixing the effects of incoming signal distortions and degradations due to the feedback component, we did not consider the residual feedback component when computing the PESQ measure.

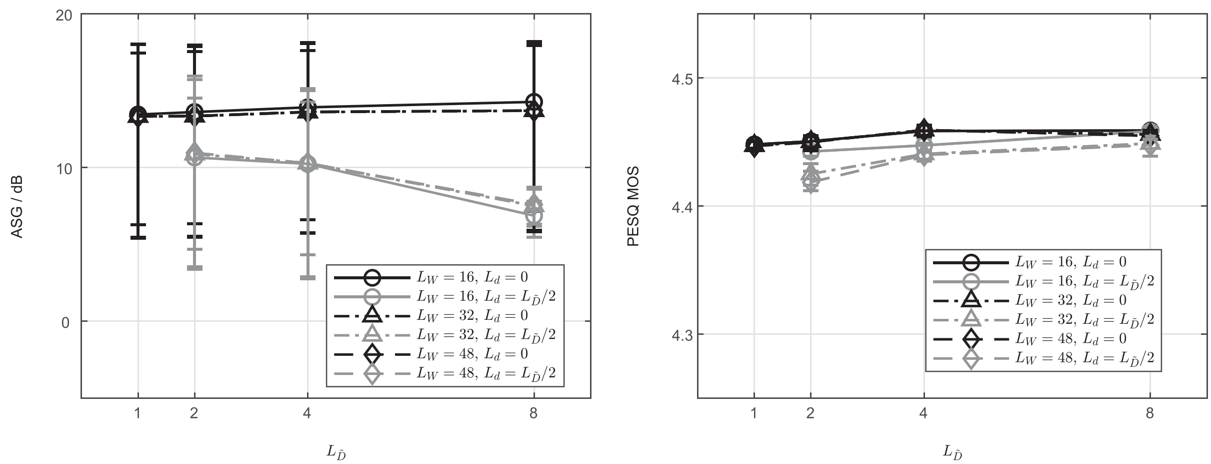

(a) ASG. (b) PESQ.

Fig. 5. Exemplary average ASG and PESQ MOS values as a function of the RTF length $L_{\tilde{D}}$ using $M = 2$ microphones. Errorbars indicate minimum and maximum ASG and PESQ MOS values, respectively.

C. Experiment 2: Optimal Feedback Cancellation Performance

In the second experiment we investigate the optimal performance, i.e., the performance for acoustic feedback paths and acoustic transfer functions that were included in the optimization of the null-steering beamformers. We consider $I = 10$ sets of acoustic feedback paths measured in free-field and a single frontal acoustic transfer function of the incoming signal ($J = 1$) resulting in a single null-steering beamformer.

Fig. 6 depicts the average ASGs across all ten acoustic feedback paths as well as the minimum and maximum ASG as a function of the null-steering beamformer length for the two constraints. Note that the perceptual quality of the incoming signal will be evaluated in detail in Experiment 4 (cf. Section V-E). As can be observed from Fig. 6 for both constraints using $M = 3$ microphones yields a larger average ASG of up to 51 dB compared to using $M = 2$ microphones of up to 29 dB, which is an expected result. Furthermore, increasing the number of beamformer coefficients L_W generally leads to a larger ASG.

When comparing the different constraints, for $M = 2$ in Fig. 6(a) the RTF-based constraint yields a lower ASG compared to the fixed delay constraint for both optimizations. When comparing the least-squares optimization and the min-max optimization for the RTF-based constraint they yield similar average ASGs of approximately 13–14 dB, while for the fixed delay constraint the least-squares optimization yields a larger average ASG compared to the min-max optimization of approximately 3–4 dB. However, note that this is in fact an expected result, since the min-max optimization maximizes the worst-case, i.e., the minimum MSG. In terms of the minimum ASG (as indicated by the lower whiskers), the min-max optimization outperforms the least-squares optimization for both constraints by approximately 3–5 dB.

For $M = 3$ in Fig. 6(b) the RTF-based constraint yields a larger average ASG of up to 51 dB compared to the fixed delay constraint (approximately up to 31 dB ASG) for both optimizations. The difference between the performance for both constraints can most likely be explained by the different solution spaces when using different constraints, where for $M = 2$ the RTF-based constraint appears to be more restrictive than the simple fixed delay constraint. Similarly as for $M = 2$, the least-squares optimization yields a larger average ASG compared to the min-max optimization, while the min-max optimization yields a larger minimum ASG compared to the least-squares optimization for both constraints.

In summary, these results indicate that, in general, the proposed null-steering beamformers computed using the least-squares optimization procedures or using the min-max optimization procedures yield very good feedback cancellation performance. In particular, in optimal conditions the null-steering beamformers significantly increase the ASG, where the least-squares optimization procedures yield a larger average ASG compared to the min-max optimization procedures, while the min-max optimization procedures yield a larger minimum ASG compared to the least-squares optimization procedures. Furthermore, using the proposed RTF-based constraint allows to significantly increase the ASG compared to the fixed delay constraint when using $M = 3$ microphones.

D. Experiment 3: Robust Feedback Cancellation Under Unknown Feedback Paths

While the optimal performance was investigated in the second experiment, which does not reflect a realistic scenario, in the third experiment we investigate the performance of the null-steering beamformers for unknown acoustic feedback paths but a known incoming signal direction. Therefore, we consider $I = 9$ sets of acoustic feedback paths measured in free-field and a single acoustic transfer function of the incoming signal in the optimization. For each of the 10 available sets of acoustic feedback paths measured in free-field a different null-steering beamformer is computed using the remaining $I = 9$ sets of acoustic feedback path measurements. To evaluate the robustness, for each of the 10 beamformers the average ASG was computed for the set of acoustic feedback paths that was not

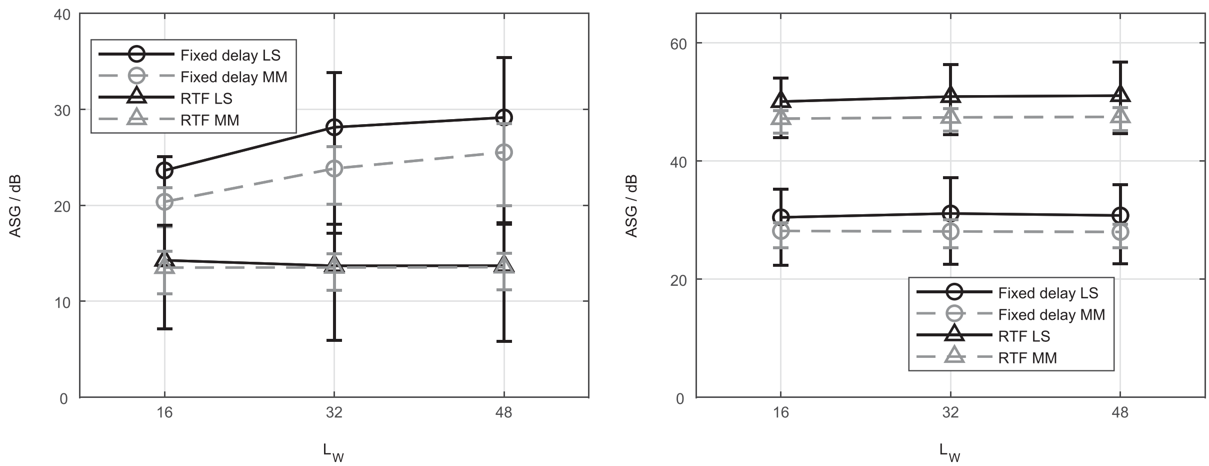

(a) $M = 2$ microphones. (b) $M = 3$ microphones.

Fig. 6. Average ASG as a function of the beamformer length L_W, showing the optimal performance (Experiment 2) for the two constraints and number of microphones. Errorbars indicate minimum and maximum ASG values.

used in the optimization, i.e., using a leave-one-out cross validation approach. However, instead of using the sets of free-field feedback path measurements for evaluation, here we used the corresponding sets of acoustic feedback paths measured with a telephone receiver in close distance. Thus, this experiment includes both variations of the sound field inside the ear canal and variations of the sound field outside of the ear.

Fig. 7 depicts the average ASGs across all ten beamformers as well as the minimum and maximum ASG as a function of the null-steering beamformer length for the two constraints as well as $M = 2$ and $M = 3$. Note that the perceptual quality of the incoming signal will be evaluated in detail in Experiment 4 (cf. Section V-E). As can be observed from Fig. 7 for both constraints using $M = 3$ microphones yields a larger average ASG of up to 41 dB compared to using $M = 2$ microphones of up to 27 dB. Furthermore, similarly as in Experiment 2 (cf. Section V-C) increasing the number of beamformer coefficients L_W again generally leads to a larger ASG.

Similarly as in Experiment 2, for $M = 2$ (cf. Fig. 7(a)) the least-squares optimization outperforms the min-max optimization in terms of the average ASG by approximately 2–3 dB. However, the min-max optimization procedures outperform the least-squares optimization procedures in terms of the minimum ASG (indicated by the lower whisker of the errorbar). For the fixed delay constraint the min-max optimization procedure leads to a minimum ASG improvement of approximately 1 dB to 2 dB compared to the least-squares optimization procedure. Similarly, for the RTF-based constraint the min-max optimization leads to a minimum ASG improvement of approximately 3 dB to 4 dB compared to the least-squares optimization procedure. Again as for the optimal case, for $M = 2$ the fixed delay constraint leads to a larger feedback cancellation performance compared to the proposed RTF-based constraint. In contrast, for $M = 3$ (cf. Fig. 7(b)) the least-squares optimization procedures outperform the min-max optimization procedures with minimum ASG improvements of approximately 1 dB to 3 dB for the fixed delay constraint and approximately 2 dB to 4 dB for the RTF-based constraint. Furthermore, the proposed RTF-based constraint yields a larger feedback cancellation performance compared to the fixed delay constraint as indicated by the largest ASG for both the least-squares optimization procedure as well as the min-max optimization procedure.

In summary, when analyzing the robustness to internal and external sound field variations, the results are mixed, where for $M = 2$ the min-max optimization procedures generally lead to the best performance, while for $M = 3$ the least-squares optimization procedures generally lead to the best performance. Hence, all optimization procedure lead to very good feedback cancellation performance, where our results indicate that depending on the number of microphones either the min-max optimization procedures (for $M = 2$) or the least-squares optimization procedures (for $M = 3$) should be chosen. Similarly, considering the feedback cancellation performance for $M = 2$ the fixed delay constraint should be chosen, while for $M = 3$ the proposed RTF constraint should be chosen.

E. Experiment 4: Preservation of the Incoming Signal

In the fourth experiment we additionally investigate the impact of known and unknown signal directions, i.e., when the RTF of the incoming signal was either included (frontal direction) or not included (left, right, and back direction) in the optimization of the null-steering beamformer. Thus this experiment provides insights into the robustness of the beamformer in terms of the incoming signal preservation. We use the same ten different beamformers used in Experiment 3 and compute the PESQ MOS values for the four different incoming signal directions. Fig. 8 depicts the average PESQ MOS values for the different directions of the incoming signal and optimization procedures for $M = 2$ and $M = 3$ microphones. As can be observed, generally all null-steering beamformers have a low distortion of the incoming signal as indicated by average PESQ MOS values larger than 4.1. The results show a general trend, that using $M = 3$ is more susceptible to distortions of the incoming signal than using $M = 2$ microphones. Hence, in combination with the results from Experiment 3 this indicates a trade-off between a higher

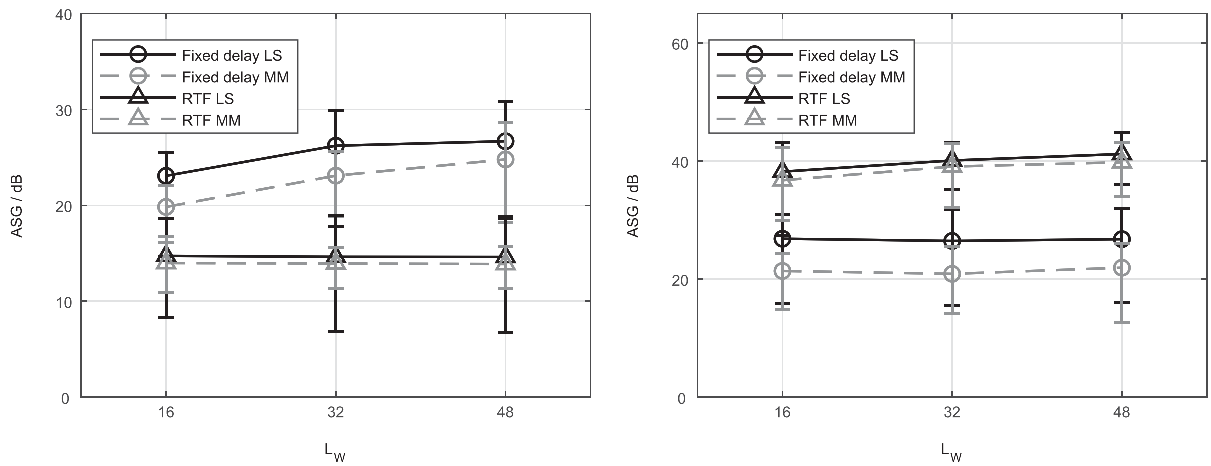

(a) $M = 2$ microphones. (b) $M = 3$ microphones.

Fig. 7. Average ASG as a function of the beamformer length L_W, showing the robust performance (Experiment 3) for the two constraints and number of microphones. Errorbars indicate minimum and maximum ASG values.

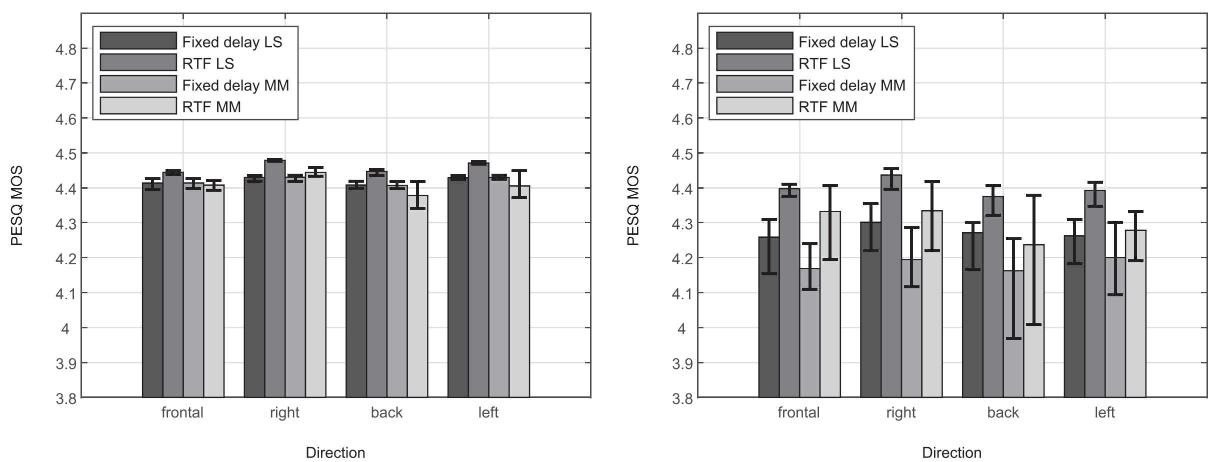

(a) $M = 2$ microphones. (b) $M = 3$ microphones.

Fig. 8. Average PESQ MOS values for different incoming signal directions and all optimization procedures using $L_W = 48$ for Experiment 4. Errorbars indicate minimum and maximum PESQ MOS values.

feedback cancellation performance for $M = 3$ and a slightly worse preservation of the incoming signal compared to using $M = 2$. Furthermore, as expected using the RTF-based constraint yields the highest perceptual quality, i.e., it preserves the incoming signal best. With average PESQ MOS values above 4.4 the least-squares optimization procedure for both $M = 2$ and $M = 3$ yields a better preservation of the incoming signal compared to the min-max optimization procedure with average PESQ MOS values above 4.3.

In summary, these results show that using the proposed RTF-based constraint in the null-steering beamformer optimization yields a large robust reduction of the acoustic feedback without distorting the incoming signal.

F. Experiment 5: Comparison and Combination With an AFC Algorithm

While using a fixed null-steering beamformer yields a large and robust acoustic feedback reduction, a further reduction can be achieved by using an additional adaptive feedback cancellation algorithm [31], see Fig. 9. The aim of the adaptive feedback canceller $\hat{H}(q)$ of length $L_{\hat{H}}$ is to reduce the residual feedback component $\tilde{f}[k] = \mathbf{W}^T(q)\mathbf{f}[k]$ in the beamformer output signal $e[k]$. In the following we compare the performance of

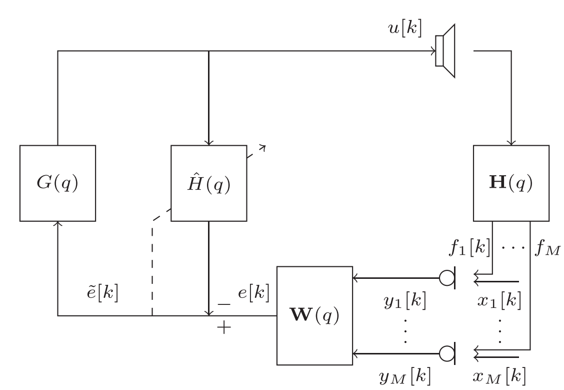

Fig. 9. Single-loudspeaker multi-microphone hearing aid system using a fixed null-steering beamformer and an AFC algorithm considered in Experiment 5.

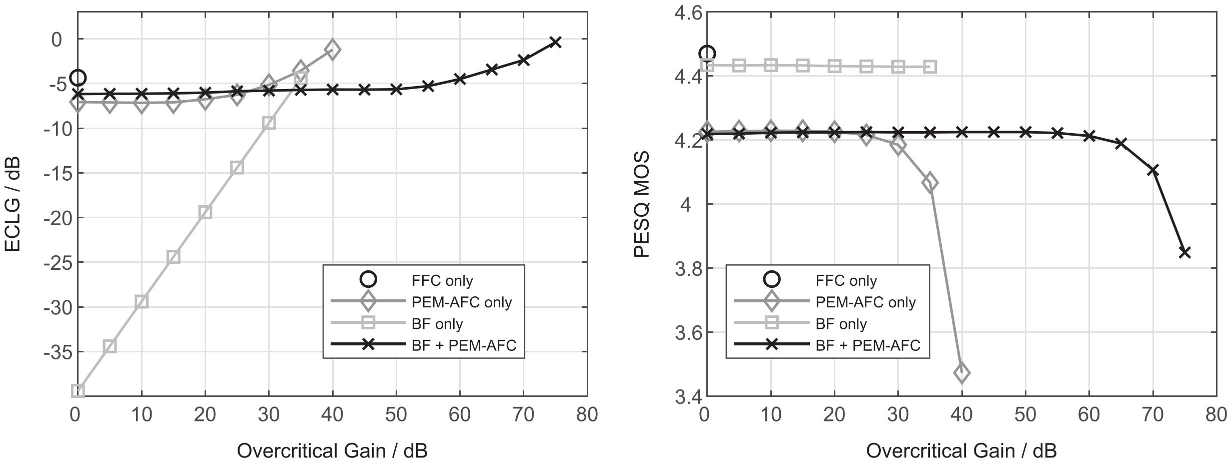

(a) ECLG.
(b) PESQ.

Fig. 10. Median ECLG and PESQ MOS values for the last 30 s of the incoming signal in Experiment 5.

combining a null-steering beamformer and the PEM-AFC algorithm [2] with using only the PEM-AFC and using only a fixed null-steering beamformer. Note that the computational complexity for the PEM-AFC algorithm is larger than for a (time-invariant) fixed null-steering beamformer due to the adaptation of the filter coefficients. We therefore also include a comparison with a fixed feedback cancellation filter.

Specifically, we consider a null-steering beamformer from Experiment 3 (cf. Section V-D), computed using the RTF-constrained least-squares optimization procedure for $M = 3$ microphones and $L_W = 32$. For the PEM-AFC algorithm we consider a fullband adaptive filter using the normalized least-mean-squares (NLMS) algorithm with a length of $L_{\hat{H}} = 64$, a step-size of $\mu = 0.002$ and a regularization constant of $\alpha = 10^{-6}$. The prewhitening filter for the PEM-AFC is of order $N_{\hat{A}} = 20$ and updated every 10 ms using the most recent 10 ms of the error signal $\tilde{e}[k]$ using the Levinson-Durbin recursion [34]. When using only the PEM-AFC algorithm we only consider the reference microphone m_0, i.e., $e[k] = y_{m_0}[k]$. The fixed feedback cancellation (FFC) filter is computed as the common all-zero filter of length $L_{\hat{H}} = ML_W$ using the optimization procedure in [32] from the acoustic feedback paths of the reference microphone m_0 of the same sets of measurements used to compute the fixed null-steering beamformer. Note that this fixed feedback cancellation filter represents the average acoustic feedback path as suggested in [33].

As the incoming signal we use the same 80 s long speech signal as described in Section V-A, played back from the right side of the dummy head. Note that this direction was not included in the optimization of the null-steering beamformer. Similarly as in Experiment 3 (cf. Section V-D) we used a set of acoustic feedback path measurements where a telephone receiver was in close distance to the dummy head (not included in the optimization of the null-steering beamformer). The forward path of the hearing aid was set to $G(q) = |G(q,k)|q^{-d_G}$, with $d_G = 96$ corresponding to a delay of 6 ms, and $|G(q,k)| = 10^{G_0(q,k)/20}$ the magnitude of the time-varying broadband gain. During the first 40 s the gain $G_0(q,k)$ was linearly increased from MSG_{m_0} to $MSG_{m_0} + \tilde{G}_0$, with $\tilde{G}_0$ the overcritical gain, and then kept constant for the remaining 40 s.

For evaluation we use the PESQ measure with $\tilde{e}[k]$ and $x_{m_0}[k]$ as test and reference signals, respectively, as well as the median across time of the effective closed-loop gain (ECLG) for the last 30 s of the speech signal. The ECLG is defined as the difference between the gain of the hearing aid and the MSG of the considered algorithm [6], [31] and can be interpreted as the gain margin that is still available until instability occurs. A hearing aid system can hence be considered stable for an $ECLG < 0$ dB.

Fig. 10 depicts the median ECLG and the PESQ MOS values for different overcritical broadband gains $\tilde{G}_0$. The median ECLG results in Fig. 10(a) show that for the PEM-AFC algorithm the closed-loop system remains stable for overcritical gains $\tilde{G}_0$ of up to 40 dB as indicated by an $ECLG < 0$. Similarly, when using the fixed null-steering beamformer the system remains stable for overcritical gains of up to 35 dB. When combining the fixed null-steering beamformer and the PEM-AFC algorithm, the system remains stable for overcritical gains of up to 85 dB, showing the benefit of the combination. Note that, when using a FFC filter, the performance is limited (the ASG is about 4 dB).

The PESQ MOS values in Fig. 10(b) show that for all considered algorithms scores of 4.2 or higher are obtained when the overcritical gain is not too large, i.e., when the $ECLG < -4$ dB (cf. Fig. 10(a)). Furthermore, it can be observed that when the $ECLG < -4$ dB fixed processing (i.e., a FFC filter or a fixed null-steering beamformer) yields the highest PESQ MOS values above 4.4, while adaptive processing yields slightly lower PESQ MOS values. When approaching higher overcritical gains and thus smaller stability margins, i.e., overcritical gains $\tilde{G}_0 > 35$ dB for the PEM-AFC algorithm and $\tilde{G}_0 > 65$ dB for the combination of the null-steering beamformer and the PEM-AFC algorithm, respectively, the PESQ MOS values decrease further due to artifacts introduced by the adaptive algorithm.

In summary, these results clearly show that using a combination of a fixed null-steering beamformer and the PEM-AFC algorithm yields an increased performance compared to using only a fixed null-steering beamformer or using only the PEM-AFC algorithm. Furthermore, the results indicate that the performance of the null-steering beamformer and the adaptive filter are complementary, i.e., the increase in performance of the combination can be explained by the individual performances. Moreover, a fixed null-steering beamformer yields a higher feedback cancellation performance compared to the considered FFC filter which has a similar computational complexity.

VI. Conclusion

In this paper we considered to use a fixed null-steering beamformer for acoustic feedback cancellation in a custom multi-microphone hearing aid. In contrast to previous approaches that used a fixed delay constraint, in this paper we proposed to use a constraint based on the RTF of the incoming signal which allows to directly preserve the incoming signal in the beamformer output. We showed how this RTF constraint can be incorporated when either minimizing the residual feedback power, leading to a linearly constrained least-squares optimization problem, or maximizing the MSG of the hearing aid, leading to a linearly constrained min-max optimization problem. In order to minimize the linearly constrained min-max optimization, we proposed to apply the real rotation theorem, leading to a linearly constrained LP. Experimental results using measured acoustic impulse responses and acoustic transfer functions from a custom earpiece with three microphones show that using the proposed RTF-based constraint yields a lower distortion of the incoming signal compared to the fixed delay constraint, even if the incoming signal direction was not considered in the optimization. Furthermore, when all three microphones were used, the RTF-based constraint yields the largest ASG of up to 41 dB even for unknown acoustic feedback paths that were not included in the optimization. A comparison of the two different objective functions used for optimization, i.e., minimizing the residual feedback power and maximizing the MSG, shows that depending on the number of microphones either of the two objective functions can be used to compute a robust null-steering beamformer when using the proposed RTF-based constraint. Furthermore, experimental results show that using a combination of a fixed null-steering beamformer and a PEM-AFC algorithm yields a larger ASG compared to using only a fixed null-steering beamformer or using only the PEM-AFC algorithm.

Appendix
Computation of RTFs

The RTFs $\tilde{\mathbf{d}}_m$, $m = 1, \ldots, M$ in this paper are computed by minimizing the squared norm between the delayed acoustic transfer function in each microphone and the filtered acoustic transfer function in the reference microphone m_0, i.e., minimizing the following least-squares optimization problem

$$\min_{\tilde{\mathbf{d}}_{m_0}} \quad \|\mathbf{D}_{m_0}\tilde{\mathbf{d}}_m - \check{\mathbf{d}}_m\|_2^2, \tag{56}$$

where $\mathbf{D}_{m_0}$ is the $(L_D + L_{\tilde{D}} + L_d - 1) \times L_{\tilde{D}}$-dimensional convolution matrix of $\mathbf{d}_{m_0}$ and $\check{\mathbf{d}}_m$ the L_d samples delayed vector of $\mathbf{d}_m$ defined as

$$\check{\mathbf{d}}_m = [\underbrace{0 \quad \ldots \quad 0}_{L_d} \quad \mathbf{d}_m]^T. \tag{57}$$

The solution to the optimization problem is given as

$$\tilde{\mathbf{d}}_m = (\mathbf{D}_{m_0}^T\mathbf{D}_{m_0} + \epsilon\mathbf{I})^{-1}\mathbf{D}_{m_0}^T\check{\mathbf{d}}_m, \tag{58}$$

where we included a small regularization constant $\epsilon = \frac{10^{-6}}{L_{\tilde{D}}}\mathrm{trace}(\mathbf{D}_{m_0}^T\mathbf{D}_{m_0})$ to avoid numerical problems.

References

[1] T. van Waterschoot and M. Moonen, “Fifty years of acoustic feedback control: State of the art and future challenges,” *Proc. IEEE*, vol. 99, no. 2, pp. 288–327, Feb. 2011.

[2] A. Spriet, I. Proudler, M. Moonen, and J. Wouters, “Adaptive feedback cancellation in hearing aids with linear prediction of the desired signal,” *IEEE Trans. Signal Process.*, vol. 53, no. 10, pp. 3749–3763, Oct. 2005.

[3] A. Spriet, S. Doclo, M. Moonen, and J. Wouters, “Feedback control in hearing aids,” in *Springer Handbook of Speech Processing*. Berlin, Germany: Springer-Verlag, 2008, pp. 979–999.

[4] M. Guo, S. H. Jensen, and J. Jensen, “Novel acoustic feedback cancellation approaches in hearing aid applications using probe noise and probe noise enhancement,” *IEEE Trans. Audio, Speech, Lang. Process.*, vol. 20, no. 9, pp. 2549–2563, Nov. 2012.

[5] C. R. C. Nakagawa, S. Nordholm, and W.-Y. Yan, “Feedback cancellation with probe shaping compensation,” *IEEE Signal Process. Lett.*, vol. 21, no. 3, pp. 365–369, Mar. 2014.

[6] F. Strasser and H. Puder, “Adaptive feedback cancellation for realistic hearing aid applications,” *IEEE/ACM Trans. Audio, Speech, Lang. Process.*, vol. 23, no. 12, pp. 2322–2333, Dec. 2015.

[7] H. Schepker, L. T. T. Tran, S. Nordholm, and S. Doclo, “Improving adaptive feedback cancellation in hearing aids using an affine combination of filters,” in *Proc. Int. Conf. Acoust., Speech, Signal Process.*, Shanghai, China, Mar. 2016, pp. 231–235.

[8] S. Nordholm, H. Schepker, L. T. T. Tran, and S. Doclo, “Stability-controlled hybrid adaptive feedback cancellation scheme for hearing aids,” *J. Acoust. Soc. Amer.*, vol. 143, no. 1, pp. 150–166, Jan. 2018.

[9] M. G. Siqueira and A. Alwan, “Steady-state analysis of continuous adaptation in acoustic feedback reduction systems for hearing-aids,” *IEEE Trans. Speech Audio Process.*, vol. 8, no. 4, pp. 443–453, Jul. 2000.

[10] L. T. T. Tran, H. Schepker, S. Doclo, H. H. Dam, and S. E. Nordholm, “Proportionate NLMS for adaptive feedback cancellation in hearing aids,” in *Proc. IEEE Int. Conf. Acoust., Speech, Signal Process.*, New Orleans, LA, USA, Mar. 2017, pp. 211–215.

[11] M. Guo, S. H. Jensen, J. Jensen, and S. L. Grant, “On the use of a phase modulation method for decorrelation in acoustic feedback cancellation,” in *Proc. Eur. Signal Process. Conf.*, Bucharest, Romania, Aug. 2012, pp. 2000–2004.

[12] C. R. C. Nakagawa, S. Nordholm, and W.-Y. Yan, “Analysis of two microphone method for feedback cancellation,” *IEEE Signal Process. Lett.*, vol. 22, no. 1, pp. 35–39, Jan. 2015.

[13] L. T. T. Tran, S. Nordholm, H. Schepker, H. Dam, and S. Doclo, “Two-microphone hearing aids using prediction error method for adaptive feedback control,” *IEEE/ACM Trans. Audio, Speech, Lang. Process.*, vol. 26, no. 5, pp. 909–923, May 2018.

[14] A. Spriet, G. Rombouts, M. Moonen, and J. Wouters, “Combined feedback and noise suppression in hearing aids,” *IEEE Trans. Audio, Speech, Lang. Process.*, vol. 15, no. 6, pp. 1777–1790, Aug. 2007.

[15] G. Rombouts, A. Spriet, and M. Moonen, “Generalized sidelobe canceller based combined acoustic feedback- and noise cancellation,” *Signal Process.*, vol. 88, no. 3, pp. 571–581, Mar. 2008.

[16] H. Schepker, L. T. T. Tran, S. Nordholm, and S. Doclo, “Acoustic feedback cancellation for a multi-microphone earpiece based on a null-steering beamformer,” in *Proc. Int. Workshop Acoust. Signal Enhancement*, Xi’an, China, Sep. 2016, pp. 1–5.

[17] H. Schepker, L. T. T. Tran, S. Nordholm, and S. Doclo, “A robust average null-steering beamformer for acoustic feedback cancellation for a multi-microphone earpiece,” in *Proc. ITG Conf. Speech Commun.*, Paderborn, Germany, Oct. 2016, pp. 165–169.

[18] H. Schepker, L. T. T. Tran, S. E. Nordholm, and S. Doclo, "Null-steering beamformer for acoustic feedback cancellation in a multi-microphone earpiece optimizing the maximum stable gain," in *Proc. IEEE Int. Conf. Acoust., Speech, Signal Process.*, New Orleans, LA, USA, Mar. 2017, pp. 341–345.

[19] F. Denk, M. Hiipakka, B. Kollmeier, and S. M. A. Ernst, "An individualized acoustically transparent earpiece for hearing devices," *Int. J. Audiol.*, vol. 57, no. S3, pp. S62–S70, Jun. 2018.

[20] F. Denk, S. Vogl, H. Schepker, B. Kollmeier, M. Blau, and S. Doclo, "The acoustically transparent hearing device: Towards integration of individualized sound equalization, electro-acoustic modeling and feedback cancellation," in *Proc. Int. Workshop Challenges Hearing Assistive Technol.*, Stockholm, Sweden, Aug. 2017, pp. 89–94.

[21] R. L. Streit and A. H. Nuttall, "A general Chebyshev complex function approximation procedure and an application to beamforming," *J. Acoust. Soc. Amer.*, vol. 72, no. 1, pp. 181–190, Jul. 1982.

[22] H. Schepker and S. Doclo, "A semidefinite programming approach to min-max estimation of the common part acoustic feedback paths in hearing aids," *IEEE/ACM Trans. Audio, Speech, Lang. Process.*, no. 24, vol. 2, pp. 366–377, Feb. 2016.

[23] S. P. Boyd and L. Vandenberghe, *Convex Optimization*. Cambridge, U.K.: Cambridge Univ. Press, 2004.

[24] A. H. Sayed, *Fundamentals of Adaptive Filtering*. Hoboken, NJ, USA: Wiley, 2003.

[25] M. Grant and S. Boyd, "Graph implementations of nonsmooth convex programs," in *Recent Advances in Learning and Control* (Lecture Notes in Control and Information Sciences). V. Blondel, S. Boyd, and H. Kimura, Eds. Berlin, Germany: Springer-Verlag, 2008, pp. 95–110.

[26] M. Grant and S. Boyd, "CVX: Matlab software for disciplined convex programming, version 2.1," Dec. 2016. [Online]. Available: http://cvxr.com/cvx

[27] M. Hiipakka, M. Tikander, and M. Karjalainen, "Modeling the external ear acoustics for insert headphone usage," *J. Audio Eng. Soc.*, vol. 58, no. 4, pp. 269–281, Apr. 2010.

[28] "Perceptual evaluation of speech quality (PESQ), an objective method for end-to-end speech quality assessment of narrowband telephone networks and speech codecs," International Telecommunication Union, Geneva, Switzerland, ITU-T Recommendation P.862, 2001.

[29] J. M. Kates, "Room reverberation effects in hearing aid feedback cancellation," *J. Acoust. Soc. Amer.*, vol. 109, no. 1, pp. 367–378, Jan. 2001.

[30] J. S. Garofolo, "Getting started with the DARPA TIMIT CD-ROM: An acoustic phonetic continuous speech database," Nat. Inst. Standards Technol., Gaithersburg, MD, USA, Dec. 1988.

[31] H. Schepker, L. T. T. Tran, S. E. Nordholm, and S. Doclo, "Combining null-steering and adaptive filtering for acoustic feedback cancellation in a multi-microphone earpiece," in *Proc. Eur. Signal Process. Conf.*, Kos Island, Greece, Aug. 2017, pp. 241–245.

[32] H. Schepker and S. Doclo, "Least-squares estimation of the common pole-zero filter of acoustic feedback paths in hearing aids," *IEEE Trans. Audio, Speech, Lang. Process.*, vol. 24, no. 8, pp. 1334–1347, Aug. 2016.

[33] B. D. Woodruff and D. A. Preves, "Fixed filter implementation of feedback cancellation for in-the-ear hearing aids," in *Proc. Workshop Appl. Signal Process. Audio Acoust.*, New Paltz, NY, USA, Oct. 1995, pp. 22–23.

[34] J. Benesty, J. Chen, and Y. Huang, "Linear prediction," in *Springer Handbook of Speech Processing*. Berlin, Germany: Springer-Verlag, 2008, pp. 979–999.

Henning Schepker (S'14–M'19) received the B.Eng. degree from Jade University of Applied Sciences, Oldenburg, Germany, in 2011, and the M.Sc. degree (with distinction) from the University of Oldenburg, Oldenburg, Germany, in 2012, both in hearing technology and audiology, and the Dr.-Ing. degree from the University of Oldenburg, in 2017. He is currently a Postdoctoral Researcher with the Signal Processing Group, Department of Medical Physics and Acoustics, University of Oldenburg. His research interests are in the area of signal processing for hearing devices and speech and audio applications as well as speech perception.

Sven Erik Nordholm (SM'04) received the MScEE (Civilingenjör) degree in 1983, Licentiate of Engineering degree in 1989, and the Ph.D. degree in signal processing in 1992 all from Lund University, Lund, Sweden.

Since 1999, he has been a Professor in signal processing with the Department of Electrical and Computer Engineering, Curtin University, Bentley, WA, Australia. From 1999 to 2002, he was a Director of ATRI. From 2002 to 2009, he was a Director of the Signal Processing Laboratory, Western Australian Telecommunication Research Institute, a joint institute between The University of Western Australia and Curtin University. He is a co-founder of two start-up companies: Sensear, providing voice communication in extreme noise conditions, and Nuheara, a hearables company. He has written more than 200 papers in refereed journals and conference proceedings. He contributes frequently in book chapters and encyclopedia articles and is the Editor of two special issues on hearing aids and microphone arrays. He is holding seven patents in the area of speech enhancement and microphone arrays. His main research efforts have been spent in the fields of speech enhancement, adaptive and optimum microphone arrays, audio signal processing, and acoustic communication. He is an Associate Editor for the IEEE/ACM TRANSACTIONS ON AUDIO, SPEECH, AND LANGUAGE PROCESSING.

Linh Thi Thuc Tran (S'15) received the B.Sc. degree in electronics and telecommunications from Hanoi University of Technology, Hanoi, Vietnam, in 1999, the M.Sc. degree in digital communications from the University of Kiel, Kiel, Germany, in 2005, and the Ph.D. degree in electrical and computer engineering from Curtin University, Perth, WA, Australia, in 2018. Her research interests include acoustic feedback control and signal processing, specifically for hearing-aid applications.

Simon Doclo (S'95–M'03–SM'13) received the M.Sc. degree in electrical engineering and Ph.D. degree in applied sciences from the Katholieke Universiteit Leuven, Leuven, Belgium, in 1997 and 2003, respectively. From 2003 to 2007, he was a Postdoctoral Fellow with the Research Foundation Flanders, Electrical Engineering Department, Katholieke Universiteit Leuven, and the Cognitive Systems Laboratory, McMaster University, Hamilton, ON, Canada. From 2007 to 2009, he was a Principal Scientist with the Sound and Acoustics Group, NXP Semiconductors, Leuven, Belgium. Since 2009, he has been a Full Professor with the University of Oldenburg, Oldenburg, Germany, and Scientific Advisor for the project group Hearing, Speech, and Audio Technology with the Fraunhofer Institute for Digital Media Technology, Ilmenau, Germany. His research activities center around signal processing for acoustical and biomedical applications, more specifically microphone array processing, speech enhancement, active noise control, acoustic sensor networks, and hearing-aid processing. He was the recipient of the Master Thesis Award of the Royal Flemish Society of Engineers in 1997, the Best Student Paper Award at the International Workshop on Acoustic Echo and Noise Control in 2001, the EURASIP Signal Processing Best Paper Award in 2003 (with M. Moonen), and the IEEE Signal Processing Society 2008 Best Paper Award (with J. Chen, J. Benesty, and A. Huang). He is a member of the IEEE Signal Processing Society Technical Committee on Audio and Acoustic Signal Processing, the EURASIP Special Area Team on Acoustic, Speech, and Music Signal Processing, and the EAA Technical Committee on Audio Signal Processing. He was and is involved in several large-scale national and European research projects (ITN DREAMS, Cluster of Excellence Hearing4All, CRC Hearing Acoustics). He was the Technical Program Chair of the IEEE Workshop on Applications of Signal Processing to Audio and Acoustics in 2013 and the Chair of the ITG Conference on Speech Communication in 2018. In addition, he was a Guest Editor for several special issues (IEEE SIGNAL PROCESSING MAGAZINE, Elsevier *Signal Processing*) and is an Associate Editor for the IEEE/ACM TRANSACTIONS ON AUDIO, SPEECH, AND LANGUAGE PROCESSING and *EURASIP Journal on Advances in Signal Processing*.